





Article

Synthesis and Characterization of SiO₂ Nanoparticles for Application as Nanoadsorbent to Clean Wastewater

Nora Elizondo-Villarreal ^{1,*}, Eleazar Gandara-Martínez ^{1,*}, Manuel García-Méndez ¹, Miguel Gracia-Pinilla ¹, Ana María Guzmán-Hernández ², Víctor M. Castaño ³ and Cristian Gómez-Rodríguez ⁴

- ¹ Physical Mathematical Scientific Research Center (CICFIM), Universidad Autónoma de Nuevo León, Cd. Universitaria, San Nicolás de los Garza 66455, Nuevo León, Mexico; manuel.garciamnd@uanl.edu.mx (M.G.-M.); miguel.graciapl@uanl.edu.mx (M.G.-P.)
- ² Materials Engineering Department, Universidad Autónoma de Nuevo León, Cd. Universitaria, San Nicolás de los Garza 66455, Nuevo León, Mexico; anmgh@yahoo.com
- ³ Centro de Física Aplicada y Tecnología Avanzada, Universidad Nacional Autónoma de México, Juriquilla 76230, Querétaro, Mexico; victor.m.castano@gmail.com
- ⁴ Faculty of Engineering, University of Veracruz (Coatzacoalcos), Av. Universidad km 7.5 Col. Santa Isabel, Coatzacoalcos 96535, Veracruz, Mexico; crisgomez@uv.mx
- * Correspondence: nelizond@yahoo.com (N.E.-V.); ele-gr@hotmail.com (E.G.-M.)

Abstract: By way of the sol–gel chemical synthesis method, it is possible to synthesize SiO₂ nanoparticles with a defined specific particle size, a surface area, and a defined crystal structure that can be effectively used as a nanoadsorbent to remove various organic dyes. SiO₂ nanoparticles were synthesized by the sol–gel method using sodium silicate (Na₂SiO₃) by a green method without using a tetraethyl orthosilicate (TEOS) precursor, which is very expensive and highly toxic. This sol–gel process involves the formation of a colloidal suspension (sol) and solid gelation to form a network in a continuous liquid phase (gel). In addition, it requires controlled atmospheres. XRD indicates the presence of an amorphous phase with a diffraction angle of $2\theta = 23^\circ$, associated with SiO₂. UV-Vis spectroscopy reveals an absorbance value in the region of 200 nm to 300 nm, associated with SiO₂ nanoparticles. The application as a nanoadsorbent to remove dyes was measured, and it was found that the nanoparticles with the best performance were those that were synthesized with pH 7, showing a 97% removal with 20 mg of SiO₂ nanoparticles in 60 min. Therefore, SiO₂ nanoparticles can be used as a nanoadsorbent, using a low-cost and scalable method for application to remove methylene blue in an aqueous medium.

Keywords: SiO₂; nanoadsorbent; sol–gel; cleaning; wastewater



Citation: Elizondo-Villarreal, N.; Gandara-Martínez, E.; García-Méndez, M.; Gracia-Pinilla, M.; Guzmán-Hernández, A.M.; Castaño, V.M.; Gómez-Rodríguez, C. Synthesis and Characterization of SiO₂ Nanoparticles for Application as Nanoadsorbent to Clean Wastewater. *Coatings* **2024**, *14*, 919. <https://doi.org/10.3390/coatings14070919>

Academic Editors: Shoufeng Tang and Deling Yuan

Received: 7 June 2024
Revised: 12 July 2024
Accepted: 14 July 2024
Published: 22 July 2024



Copyright: © 2024 by the authors. Licensee MDPI, Basel, Switzerland. This article is an open access article distributed under the terms and conditions of the Creative Commons Attribution (CC BY) license (<https://creativecommons.org/licenses/by/4.0/>).

1. Introduction

Nanoparticles have received considerable attention for creating new materials or new compounds, all at the nanometer scale, with amazing new properties for developing innovative applications with great potential, so they are explored for application in industries such as the environment, water, food, biomedical, and space industries [1]. One of the applications that have the most direct impact on the development of humanity is nanoadsorbents, which can transform toxic substances into non-toxic ones since they can adsorb toxic substances by ion exchange, ion precipitation, or adsorption. Metal oxides such as TiO₂, Al₂O₃, ZrO₂, SiO₂, and ZnO have a very high adsorption capacity and are commonly used as nanoadsorbents. In particular, amorphous metal oxides are used because they have high adsorption capabilities due to their extremely high surface areas [2]. The application of nanotechnology in wastewater treatment is highly feasible due to the following characteristics of nanomaterials: (a) highly specific surface area, (b) rapid dissolution, (c) high reactivity, and (d) strong absorption of nanoparticles, all of which are used for efficient water purification [3].

Silica nanoparticles (SNPs) have shown great applicability potential in several fields like chemical, biomedical, biotechnology, agriculture, environmental remediation, and even wastewater purification. With remarkably instinctive properties like mesoporous structure, high surface area, tunable pore size/diameter, biocompatibility, modifiability, and polymeric hybridizability, SNPs are growing in their applicable potential even further. These particles are shown to be non-toxic and, hence, safe to be used in biomedical research [4].

Adsorption using different adsorbents is seen as the most effective method of treating wastewater contaminated by heavy metal ions such as copper ions. In particular, nanoadsorbents have emerged as state-of-the-art materials for heavy metal removal because of their unique physicochemical properties. The best results were obtained by the modification/functionalization of the nanoadsorbents with other materials, which increased their specific surface area. Effective treatment of copper-contaminated wastewater can be achieved with the use of nanoadsorbents as a novel, non-toxic, and cost-effective technique of adsorption [5].

Some techniques are also being developed for wastewater treatment using nanotechnology based on adsorption and biosorption, nanofiltration, photocatalysis, disinfection, and detection technology. In addition, the destination of nanomaterials in wastewater treatment is highlighted, along with the risks associated with their use [6].

There are two main sources of wastewater: residential and non-residential sources. Residential wastewater consists of waste products discharged from undigested food materials in the body, which are diluted by approximately 99%. In addition to water, wastewater also contains approximately 1% of solid particles that can be classified as organic and inorganic [7]. Organic materials in wastewater include carbohydrates, proteins, and lipids, while inorganic materials include sediments, salts, and metals.

Non-residential wastewater is the waste released from commercial, industrial, and agricultural operations; these are the wastewaters that are much more polluted, and it is in these waters where the most work is required so that they can be reused. Different types of commercial or industrial sectors are responsible for the various wastewater components. The sectors that generate the most water pollution are (1) the textile industries which mainly release dyes and synthetic chemicals and (2) the agricultural sector with wastewater containing pesticides, insecticides, and fertilizers [8].

The dyes used in the textile industry are some of the main pollutants to be eliminated from wastewater. Many dyes are toxic, and tons of these pigments are released during dyeing and finishing operations in the textile sector. These released dyes pose environmental risks, as they can cause carcinogenic and mutagenic effects, among other harmful effects such as damage to the brain, central nervous system, and reproductive system [9]. Dyes can be divided into two types of dyes, cationic and anionic dyes depending on a negative ion. Anionic dyes, also called acid dyes, are soluble in water. The main harmful effect on humans is due to their sulfonic acids.

Cationic dyes carry a positive charge in their molecule and are soluble in water. They are found in various types of dyes, mainly in azoic dyes and methylene dyes, as well as various polycyclic and solvent dyes. Basic dyes are highly visible. Cationic dyes are widely used for modeling in dye adsorption studies, with the most used ones being methylene blue, basic blue, and basic red. The most commonly used cationic dye is methylene blue (MB), which is used not only as a dye but also as a disinfectant in other dyes, rubber, pharmaceuticals, and pesticides. It has a molecular weight of 373.9 g/mol and a maximum wavelength of 660 nm. Its molecular formula is $C_6H_{18}N_3SC$. Metal oxide nanoparticles are among the most commonly used for methylene blue degradation [10]; for example, iron oxide [11], copper oxide [12], or zinc oxide is to remove it from wastewater [13].

Absorption is carried out to polish wastewater, as it can remove organic or inorganic substances. Absorption kinetics, lack of selectivity, and active sites are factors that affect the efficiency of adsorbents. Carbon-based nanoadsorbents have desirable properties of nanomaterials, such as a high specific surface area, highly accessible adsorption sites, tunable surface chemistry, and easy reusability. Similarly, metal oxide nanoparticles have

a high specific surface area, a short particle diffusion distance, more adsorption sites, and are compressible without a significant reduction in surface area, as well as having gentle reusability properties. These particles are applied in absorption media filters and sludge reactors. Nanoadsorbents can quickly mix, facilitating the mass transfer process [14]. They have also been used for arsenic removal, proving to be more cost-effective than other techniques, although the main use of nanoadsorbents is for dye removal or degradation [15].

Silicon (Si) and oxygen (O) are the two most abundant elements in the Earth's crust. Silicon is commonly found in nature as sand in the form of quartz minerals. Additionally, due to its great abundance, it exists in many different forms that can be both crystalline and amorphous materials. Silicon can be found in nature in various forms: minerals, flint, jasper, and opal. When silicon and oxygen mix with reactive metals, the result is a class of minerals called silicates, which includes granite, feldspar, and mica. The main applications of silica are industrial, as a key ingredient in bricks, concrete, and glass [16].

SiO₂ nanoparticles can be prepared through two main methods: the Stober process [17] (using a tetraethyl orthosilicate precursor) and green synthesis [18] (although this is combined with the combustion technique, which involves high-temperature burning of the reactants [19]). The commonly used reagent for synthesizing SiO₂ nanoparticles is the organic chemical called TEOS (tetraethyl orthosilicate) [20], which is very expensive and highly toxic. In addition, it requires controlled atmospheres for both the reagents and during synthesis, leading to high production costs, high energy consumption, and environmental risks.

The development of facile synthesis routes for highly efficient nanomaterials is one of the key research areas in modern technology. Some studies demonstrate a novel and facile green synthesis of SiO₂ nanoparticles using a simple extraction and precipitation method. These green synthesis methods reduce the energy requirement in many cases. And the resulting SiO₂ nanoparticles exhibit enhanced adsorption removal efficiency for water pollutants [21].

Green synthesis offers a superior alternative to traditional methods for producing metal and metal oxide nanoparticles. This approach is not only benign and safe but also cost-effective, scalable, and straightforward, operating under ambient conditions. Notable metals and metal oxide nanoparticles, such as manganese oxides, iron oxides, silver, and gold, have been produced using various bio-reductants derived from plant extracts. These biological agents not only expedite the reduction process but also stabilize the nanoparticles, playing dual roles as reducing and capping agents. Additionally, the green synthesis of metal nanoparticles highlights their potential medical applications in areas like antiviral treatments and cancer therapy [22,23].

An alternative to avoid the use of TEOS for SiO₂ synthesis is the sol-gel process [24], which involves the formation of a colloidal suspension (sol) and solid gelation to form a network in a continuous liquid phase (gel). The parameters that affect sol-gel products are water concentration, temperature, and the catalyst, which significantly influences the time to reach a gel [25]. This chemical synthesis can be used to produce large volumes of nanomaterials. The aim of this study is to prepare and characterize SiO₂ nanoparticles using a low-cost and scalable method for the application of removing methylene blue in an aqueous medium. This study presents a novel approach in the field of nanotechnology, focusing on the preparation and characterization of SiO₂ nanoparticles using a low-cost and scalable sol-gel method for the removal of methylene blue from aqueous solutions. The key points highlighting the novelty of this study are as follows:

Alternative Synthesis Method: The study introduces the sol-gel process as an alternative to the conventional TEOS-based synthesis of SiO₂ nanoparticles. This method is not only cost-effective but also scalable, making it suitable for large-scale production.

Environmental and Economic Benefits: By avoiding the use of TEOS, which is expensive and toxic, the proposed method reduces environmental risks and production costs, contributing to more sustainable and economically viable nanoparticle synthesis.

High Efficiency in Dye Removal: The study focuses on the application of SiO₂ nanoparticles for the removal of methylene blue, a common and hazardous dye in wastewater. The effectiveness of SiO₂ nanoparticles in adsorbing and degrading this dye highlights their potential in wastewater treatment.

Characterization of SiO₂ Nanoparticles: Detailed characterization of the synthesized nanoparticles is provided, demonstrating their high specific surface area, reactivity, and adsorption capacity. These properties are critical for their application in environmental remediation.

Interdisciplinary Relevance: The study bridges material science, chemistry, and environmental engineering, showcasing an interdisciplinary approach that enhances the understanding and application of nanotechnology in real-world environmental issues.

Practical Implications: The findings suggest that SiO₂ nanoparticles can be effectively used in practical applications such as wastewater treatment, particularly for industries that release significant dye pollutants, thereby directly impacting environmental sustainability and public health.

By addressing these aspects, the study not only advances the field of nanotechnology but also provides practical solutions for environmental challenges, making it a significant contribution to both scientific research and industrial applications.

2. Materials and Methods

2.1. Synthesis of SiO₂ Nanoparticles

We diluted 14 mL of sodium silicate (Na₂SiO₃) with 11 mL of deionized water and alternately added 1 mL of 20% HCl every two minutes until a pH of 7 was attained. The total duration of this test was 34 min (15 mL of 20% HCl was added). Due to the tendency of Na₂SiO₃ to gel when in contact with HCl, it was necessary to keep the substance in a container with a small diameter (3–5 cm). This was done in order to keep the entire sample moving. Once it was free of chlorine, it was taken to the oven to dry for at least 18 h at 90 °C. Ultimately, once the material dried, it was crushed using the mortar.

After the dissolution of the reagent, deionized water was once again added to obtain a final solution with a pH of 13. The pH was further reduced by adding HCl while mixing the solution, which was performed in a container with a small diameter, every few minutes until the desired pH was achieved. This is because the pH of the solution was determined by time intervals.

2.2. X-ray Diffraction Analysis (XRD)

This analysis was performed using the X-ray diffraction method using the powder method. The phase or phases were identified by comparing the diffractograms to the patterns reported in articles pertaining to the same type of nanoparticles. The measurements were conducted with a range of 10° to 40°. X-ray diffraction patterns were obtained using a diffractometer, Rigaku MiniFlexII, using CuK α radiation ($\lambda = 1.5418 \text{ \AA}$).

2.3. UV-Vis Spectroscopy (UV-Vis)

For all samples used in the study, optical absorbance measurements were performed as a function of wavelength in a range from 200 to 600 nm using a Thermo SCIENTIFIC EVOLUTION 600 Spectrophotometer (Thermo Electron Scientific Instruments LLC, Madison, WI, USA).

2.4. Removal of Methylene Blue in Water

For the removal of methylene blue, a dye solution with a concentration of 10 mg/L was prepared, of which 50 mL was used. Six variants were made for the four samples: pH 2, pH 5, pH 7, and commercial. The first three variants were by weight, using 10, 20, and 30 mg of SiO₂ nanoparticles, and the second three were by time, using 10, 30, and 60 min, respectively.

The percentage of dye degradation was calculated using the absorbance value at 660 nm, using Equation (1):

$$\eta = \frac{C_0 - C_t}{C_0} \times 100 \quad (1)$$

where η = % degradation, C_0 is the initial concentration of the dye solution, and C_t is the concentration of the dye solution after degradation [13].

3. Results

3.1. FTIR Spectrum Analysis

Figure 1 depicts the FTIR spectrum of SiO₂ nanoparticles, highlighting the bending vibration peak of H-O-H at 1630 cm⁻¹ and the antisymmetric stretching vibration peak of the Si-O-Si group at 1090 cm⁻¹. These vibrations belong to the characteristic peak of SiO₂, indicating that the primary constituent of the sample is SiO₂. Shi et al., 2022, found a similar result, using the same sol-gel technique to synthesize SiO₂ aerogels [26].

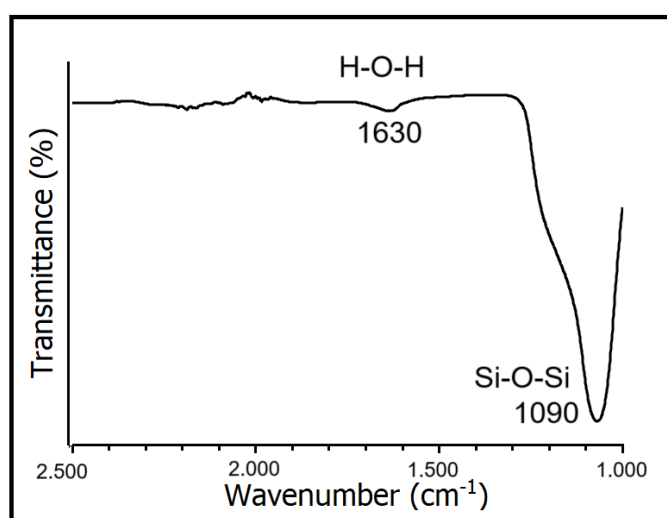


Figure 1. FTIR spectrum of SiO₂ nanoparticles.

3.2. X-ray Diffraction of SiO₂ Nanoparticles

The spectra in Figure 2 are from the pH 2, pH 5, pH 7, and commercial (COM) samples, which all have the same conditions, the only difference between them being the final pH of each synthesis. The diffraction pattern demonstrated that the nanoparticles have an amorphous nature, due to their tendency to agglomerate. In 2022, Alavi et al. [27] used the antimicrobial properties of SiO₂ nanoparticles for blood product cleaning and primarily associated them with their surface functionalization, but mentioned that agglomeration is an undesirable effect, so it is common to report their agglomeration.

Due to this, only the presence of a reflection corresponding to the diffraction angle of $2\theta = 23^\circ$ [28] is reported for SiO₂ nanoparticles and sometimes in the angle range (20 < 30) [29]. Therefore, it is observed that all samples consist of SiO₂, as they all coincide with the mentioned peak. In 2023, Mikhnenko et al. [30] studied a defective structure of NiO nanocrystals stabilized by SiO₂ nanoparticles. In their study of XRD, in the angle range (20 < 30), they found what they call a halo, and they mention that it is due to amorphous SiO₂. Although it is small compared to other different material standards, it is considered proof of identification of nano-SiO₂. In addition, with the finding of no greater intensity of the diffraction peak compared to the commercial sample in the case of commercial nanoparticles, it is determined that they are all nanoparticles of nanometer size.

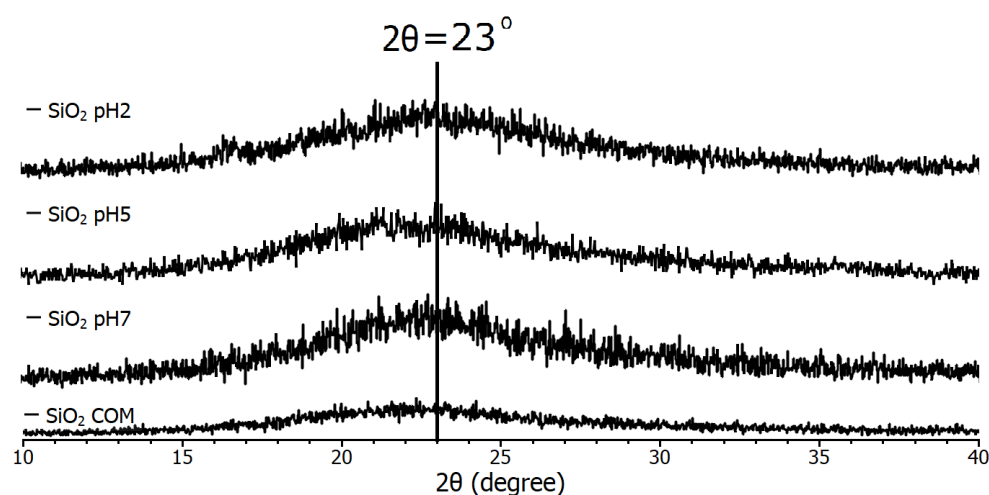


Figure 2. Diffraction pattern of SiO₂ samples used in the study.

3.3. UV-Vis of SiO₂ Nanoparticles

Figure 3 shows the absorbance spectrum curves for the commercial SiO₂, pH 2, pH 5, and pH 7 samples. In these spectra, a very similar behavior can be observed for all the values of the samples, which indicates that the nanoparticles in the study have a high absorbance value in the region of 200 nm to 300 nm, and this is also an indication that the material shows the nature of the samples. These data are similar to those found in 2022 [31] by Eissa et al. when using the same type of SiO₂ nanoparticles to see their effects on irrigation water, soil, and productivity improvements; using green chemistry, the nanoparticles exhibited an absorption peak at 208 nm, attributable to the characteristic absorption of SiO₂, identical to all the characterized samples.

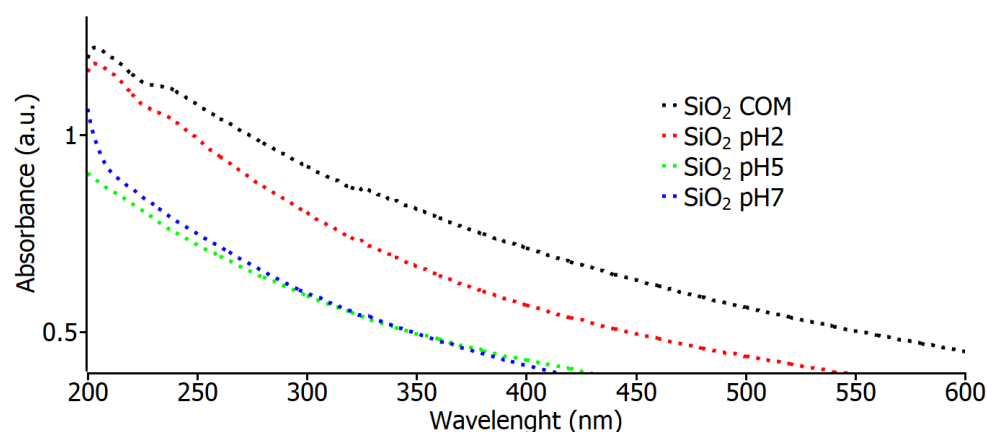


Figure 3. Optical absorbance measurements for commercial SiO₂ samples and varying pH.

3.4. SEM of SiO₂ Nanoparticles

Based on the SEM images shown in Figure 4a, we can say that SiO₂ nanoparticles form a large-size “combination” (cluster). In order to observe the clusters that can be generated in several hundred nanometers, we must use a large amount of magnification. In this particular instance, we shall examine SEM images acquired at a magnification of approximately 60,000 (with an index of 500 nm), as shown in Figure 4b. In this instance, it is feasible to observe larger nanoclusters that can be formed in nano size. It is evident that TEM images of these clusters are necessary to obtain a more precise understanding of their morphology and sizes. Moreover, in order to investigate the composition of SiO₂ nanoparticles, EDX analyses have been conducted on the samples in a scanning electron microscope (SEM) apparatus (Figure 4).

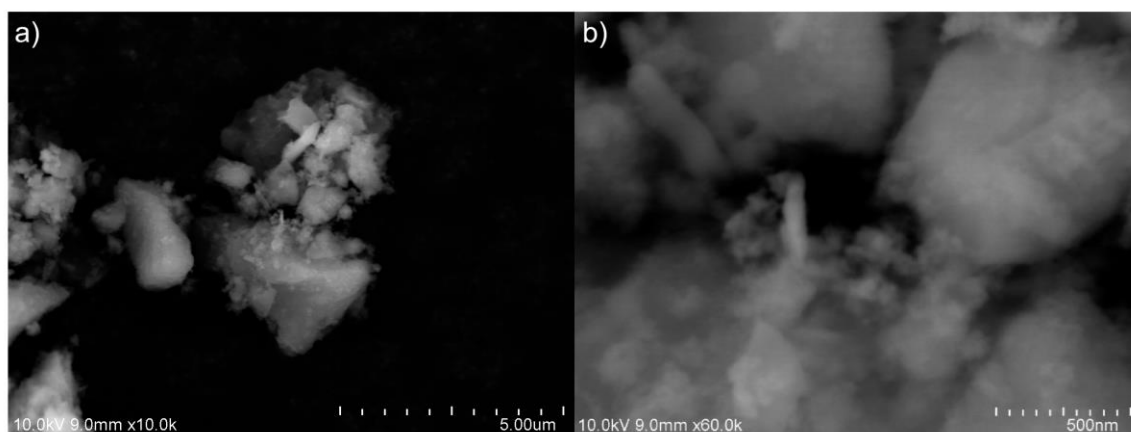


Figure 4. The scanning electron microscope (SEM) image from amorphous SiO_2 nanoparticle synthesized: (a) $\times 10.0\text{k}$ and (b) $\times 60.0\text{k}$.

3.5. Energy-Dispersive X-ray (EDX) Analysis of SiO_2 Nanoparticles

The investigated nanoparticles have undergone an energy-dispersive X-ray (EDX) analysis performed to inspect their composition. Figure 5a,b show the selected area of analysis, while the inset table shows the EDX spectrum. The EDX results confirmed the formation of SiO_2 was achieved. In Figure 5b, it can be observed that the highest peak associated with the oxygen and silicon atoms in the second peak appeared. The atomic values obtained from the EDX test are presented in the inset table as weight percentages. According to the results of the inset table of Figure 5b, nanoparticles were synthesized with a purity of 98.1%, which indicates that the method is efficient. In a similar case, in 2022, Imoisili et al. used a sol-gel hydrothermal method using fly ash to form spherical SiO_2 nanoparticles with 98% as determined by EDX [32].

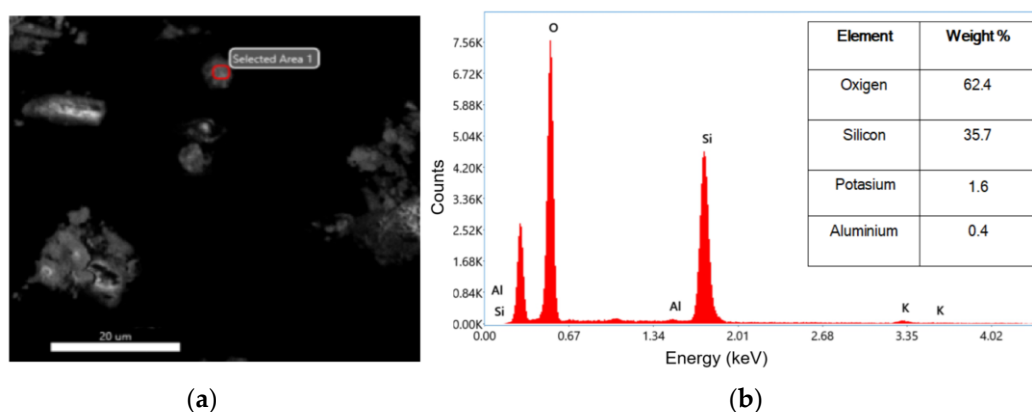


Figure 5. (a) SEM image of selected area for EDX analysis; (b) EDX analysis pattern of SiO_2 and the inset table of corresponding values of weight percentages.

3.6. TEM of SiO_2 Nanoparticles

The primary objective of performing TEM scanning is to observe the cluster of SiO_2 nanoparticles and determine their morphology and size. The TEM images were scanned with micron-size images at 20,000 and 40,000 magnification (Figures 6a and 6b, respectively). The sample consists of pure nanoparticles, but it is difficult to see a good morphology or size at this magnification for the agglomeration. Furthermore, based on the TEM image presented in Figure 6a, it can be inferred that novel nanoparticles possess a size of approximately 60 nm and exhibit an aspheric morphology. Figure 6 displays TEM images (a) and (b) of the synthesized SiO_2 nanoparticles from this study. From image (b), it is evident that the synthesized nanometer-scale SiO_2 particles are amorphous, as

no crystallinity is observed, which coincides with the X-ray diffraction results. A similar size was obtained by Rahimzadeh et al. in 2022 utilizing *Rhus coriaria* L. extract and sodium metasilicate under reflux conditions to produce SiO₂ nanoparticles; they used sodium hydroxide (NaOH) added to the mixture to control the pH of the solution, like our work, but they were using annealing at 500 °C for 40 min, while in our case, we never passed 100 °C [19]. In a similar case, in 2022, Imoisili et al., 2022 used a sol-gel hydrothermal method using fly ash to form spherical SiO₂ nanoparticles with sizes of about 60 nm [32]. To summarize the results, we present Table 1, which presents a comparison of the characteristics and descriptions of commercial and synthesized SiO₂ NPs in this work.

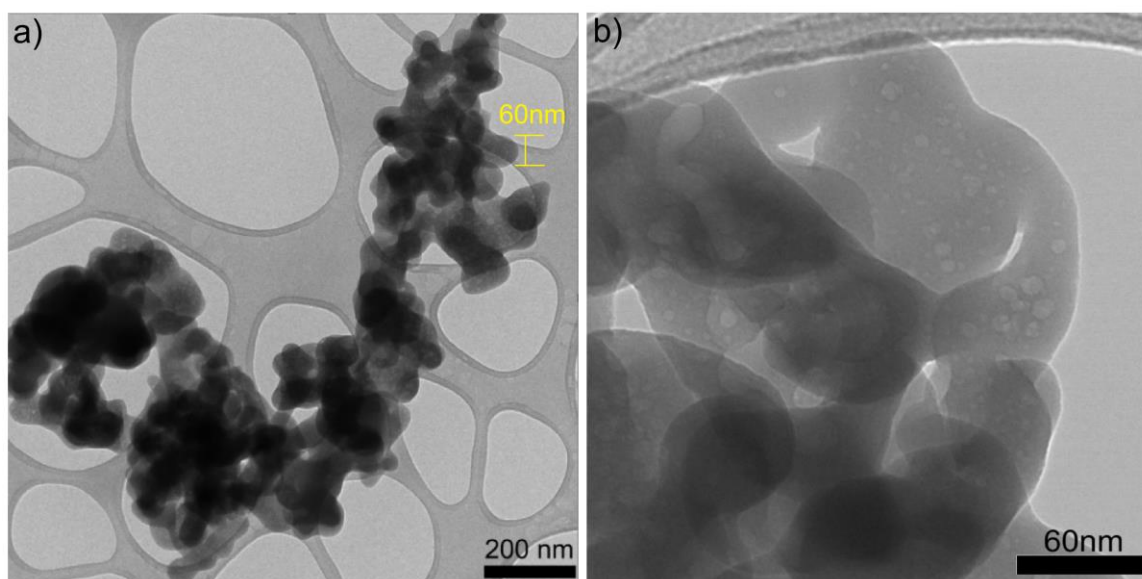


Figure 6. TEM images of SiO₂ nanoparticles at (a) $\times 20.0k$ and (b) $\times 40.0k$.

Table 1. Table of characteristics and description of commercial and synthesized SiO₂ NPs.

| Characteristic | Commercial SiO ₂ NPs | Synthesized SiO ₂ NPs |
|-----------------------|---|----------------------------------|
| Purity | 99.00% | 98.10% |
| Particle Size | 80 nm | 60 nm |
| Specific surface area | 70 m ² /g | 90 m ² /g |
| Morphology | Spherical | Spherical |
| Dispersibility | Good in aqueous and non-aqueous solvents | Good in aqueous solvents |
| Color | White powder | White powder |
| Applications | Used in coatings, electronics, drug delivery, catalysis, and more | Clean wastewater |

3.7. Methylene Blue Degradation UV-Vis

In all the measurements, the degradation of methylene blue was observed; it can only be noted that some nanoparticles are better than others, and a comparison is made with commercial ones to determine the efficiency of their use to remove the dye.

In Figure 7a, the absorbance values for the pH 2 samples with a 30 min agitation time are shown for the three different weights of SiO₂ nanoparticles. It can be observed that degradation is consistent as the nanoparticle quantity increases, with the 30 mg sample showing the highest degradation. In Figure 7b, the absorbance values for the pH 5 samples with a stirring time of 30 min are shown for the three different weights of SiO₂ nanoparticles, and it can be seen that the degradation is constant with increasing

the amount of nanoparticles, although now a similar efficiency is seen for the removal of dye from the samples with 20 and 30 mg. Figure 7c shows the absorbance spectra for commercial SiO₂ samples with 30 min stirring time for the three different nanoparticle weights. It can be seen that the degradation is constant as the amount of nanoparticles increases; the sample with 30 mg is the one that shows the most degradation, although compared to the pH 5 samples under similar conditions, the synthesized ones are more efficient, even those with lower nanoparticle content, namely the sample that has 20 mg.

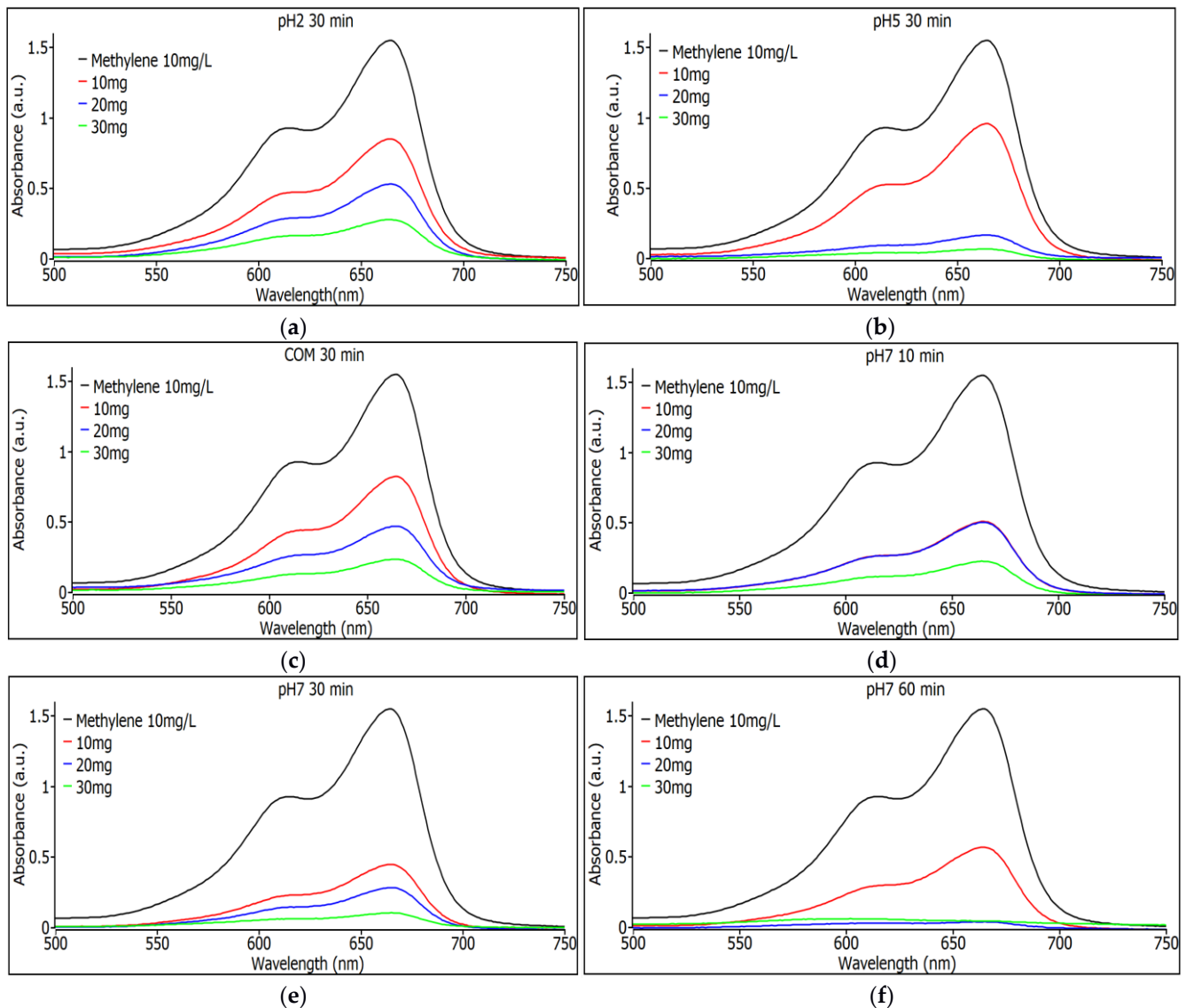


Figure 7. (a) Observance measurements for the pH 2 sample with 30 min of agitation using 10, 20, and 30 mg. (b) Observance measurements for the pH 5 sample with 30 min of shaking with 10, 20 and 30 mg. (c) Observance measurements for the commercial sample with 30 min of agitation with 10, 20 and 30 mg. (d) Observance measurements for the pH 7 sample with 10 min of shaking with 10, 20 and 30 mg. (e) Observance measurements for the pH 7 sample with 30 min of shaking with 10, 20 and 30 mg. (f) Observance measurements for the pH 7 sample with 60 min of agitation using 10, 20, and 30 mg.

Figure 7d shows the absorbance spectra for pH 7 SiO₂ samples with 10 min stirring time. For the three different nanoparticle weights, it can be seen that the degradation is constant as the amount of nanoparticles increases; the sample with 30 mg is the one that shows the most degradation, although the 10 and 20 mg samples have the same

performance indicating a saturation for the sample with 20 mg of weight. Figure 7e shows the absorbance spectra for pH 7 SiO₂ samples with 30 min stirring time. For the three different weights of nanoparticles, it can be observed that degradation remains constant as the nanoparticle quantity increases. The sample with 30 mg shows the highest degradation, although the 10 mg and 20 mg samples perform well, indicating good performance for this type of sample at pH 7. In Figure 7f, absorbance spectra are shown for SiO₂ samples at pH 7 with a 60 min agitation time for the three different nanoparticle weights. The samples with 10 and 20 mg exhibit the highest degradation among all tested samples, demonstrating superior performance compared to commercial nanoparticles.

3.8. Percentage of Methylene Blue Removal

In Table 2, we see the percentage of removal of each of the samples for each condition, using Equation (1). The commercial SiO₂ sample showed a maximum of 89% removal for the case of the highest quantity and the longest time, not reaching 90% in any of the cases.

Table 2. Percentage of methylene blue removal by sample and weight of SiO₂ nanoparticles.

| Sample/Weight NPs | 10 mg | 20 mg | 30 mg |
|-------------------|------------|------------|------------|
| COM | 10 min 38% | 10 min 66% | 10 min 77% |
| | 30 min 39% | 30 min 70% | 30 min 85% |
| | 60 min 46% | 60 min 72% | 60 min 89% |
| pH 2 | 10 min 55% | 10 min 48% | 10 min 51% |
| | 30 min 45% | 30 min 66% | 30 min 82% |
| | 60 min 67% | 60 min 51% | 60 min 83% |
| pH 5 | 10 min 34% | 10 min 64% | 10 min 92% |
| | 30 min 38% | 30 min 89% | 30 min 95% |
| | 60 min 59% | 60 min 93% | 60 min 97% |
| pH 7 | 10 min 63% | 10 min 67% | 10 min 85% |
| | 30 min 67% | 30 min 81% | 30 min 93% |
| | 60 min 80% | 60 min 97% | 60 min 97% |

The best pH 2 sample showed a maximum of 83% removal for the case of the highest amount and the longest time, and the best pH 5 sample showed a maximum of 97% removal for the case of the largest amount and the longest time, but it must be considered that more than 90% removal was reached in more than five samples, even in a sample with only 10 min of stirring. The pH 7 SiO₂ samples show the best results; although there are four that show more than 90% removal, there are two with 97% removal, and one with only 20 mg reaches 97%, showing excellent results, much better than those for commercial SiO₂ nanoparticles.

Figure 8 shows the removal measurements of commercial SiO₂ nanoparticles, showing a very similar behavior for both time and weight variations in nanoparticles, which can be explained by the size control attributed to the nanoparticles' industrial origin where equipment with high control standards is used. But even so, the commercial SiO₂ nanoparticles do not even reach a removal level of 90% in any of the variations.

Figure 9 shows the measurements of the removal of SiO₂ nanoparticles with pH 7; at 10 mg, a similar response was shown for the three times, but at 20 and 30 mg, a considerable increase can be noticed in the 60 min samples, a result that can be seen in Table 2, where 97% is shown. The highest MB removal efficiencies were found for the pH 5 and pH 7 samples for both adsorbents and were 97%. These can be explained on the basis that the pH 5 and pH 7 samples have smaller particle sizes than the commercial ones that have 80 nm, as can be seen in image 19, and therefore, they have a higher surface area, especially in the case of pH 7, which resulted in a higher adsorption capacity and a higher percentage of MB removal. The commercial SiO₂ nanometer-scale particles exhibit a very narrow distribution, whereas those synthesized in this work have a broader particle size distribution. As a result, Figures 8 and 9 illustrate different behaviors between the particles synthesized here and the

commercial ones. This variation is due to the different particle sizes, which lead to distinct degrees of adsorption. Although there are studies that mention that SiO₂ nanoparticles show photodegradation [33,34], in the study of this thesis, a different decomposition range was not found, either under darkness or under visible irradiation or under ultraviolet irradiation, so the effect of removing dyes is absorption, not photodegradation.

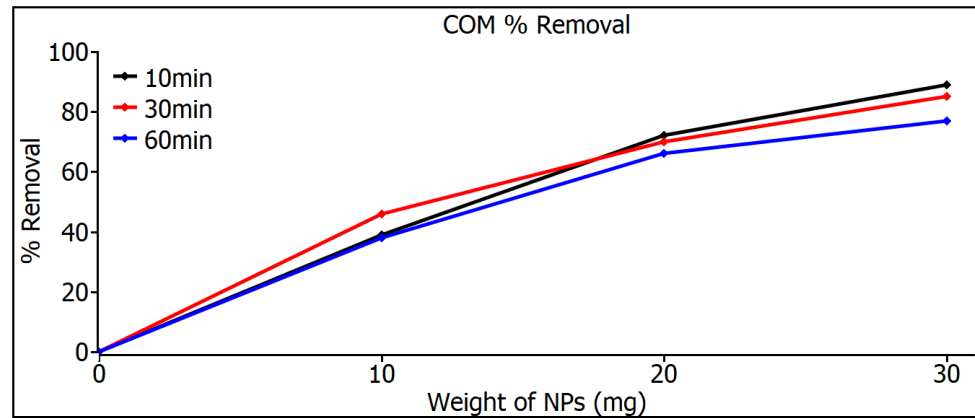


Figure 8. Removal measurements of commercial SiO₂ nanoparticles.

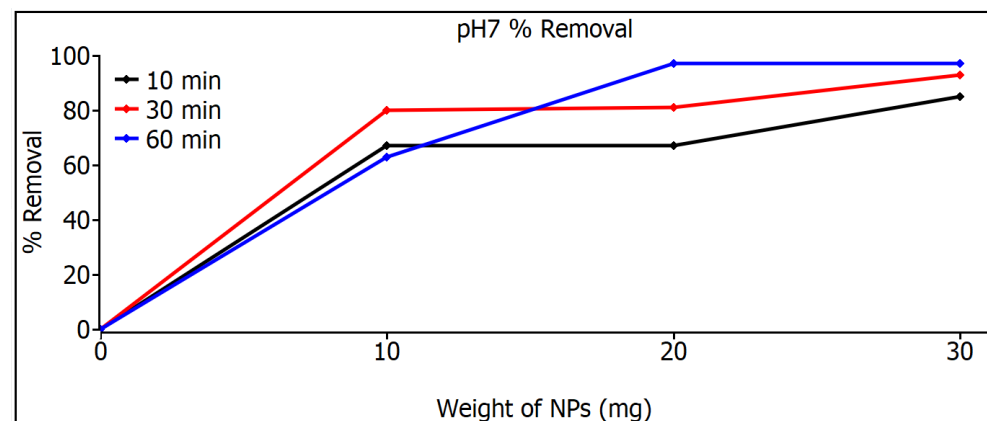


Figure 9. Removal measurements of SiO₂ nanoparticles with pH 7.

4. Discussion

Silicon dioxide (SiO₂) is an amorphous metal oxide from which nanoparticles can be obtained, exhibiting good physical and chemical properties such as adjustable size (5 nm to over 100 nm), low toxicity, biocompatibility, and a good specific surface area. These properties make them attractive and suitable for various applications in biomedicine, agriculture, catalysis, construction, and water treatment, among others [35]. Silica nanoparticles have been investigated in the field of adsorption due to their high adsorption capacity and modifiable surface. Additionally, these silica nanoparticles present silanol (Si-OH) functional groups on their surface, allowing them to interact with different compounds when they are in a solution.

The adsorption mechanism for dyes is proposed as follows: It is mainly due to surface complexation through electrostatic interactions between cationic dyes and negatively charged nanoparticles (confirmed by zeta potential measurements). Dye molecules ionize on the adsorbent surface, followed by stabilization of these charges by hydroxyl (OH) groups, which facilitate the adsorption process [36]. The adsorbent's main advantages for use as a nanoadsorbent for dye removal are that its dispersions in water and various biological media are very stable, and it has demonstrated excellent adsorption properties with a capacity of 150–200 mg/g and over 95% removal of various toxic contaminants from

water, along with reusability for more than five cycles [37]. The most common form of use for removing contaminants is in combination with other materials, combining properties and using them in dyes, such as the combination of SiO₂/TiO₂ using the hydrolysis and calcination method at 600 °C in an argon atmosphere. SiO₂ nanoparticles (11%) were used to modify TiO₂ nanoparticles, which contributed to an increase in specific surface area and total pore volume. Testing with methylene blue demonstrated that under ultraviolet irradiation, it degraded by 89%, and under visible irradiation, by 35% [38].

An interesting application would be to create SiO₂ films, but due to the nature of SiO₂, this is not feasible. However, depositing it onto a film could be a viable option. A notable application is the use of SiO₂ nanoparticles as a uranium adsorbent in the form of silica nano-meshes with a specific surface area [39]. Silicon dioxide nanoparticles are commonly used as part of the nano-oxides that have mainly been introduced into ceramic systems, proving to be an innovative alternative to improve their properties [40]. Above all, nano-SiO₂ particles as a nanomaterial are among the most widely used in concrete [41]. In other studies, the effect of adding nano-SiO₂ as an additive is sought, in order to obtain certain properties more effectively, in the material to be synthesized, especially looking at how affordable nanoparticles can be when they are made of this material [42]. A special and not-so-well-known characteristic of silica is the biocompatibility of this material with biological systems [43], which combined with good chemical stability makes it a material of great interest for many applications.

In 2022, El-Feky et al. [44] conducted a study similar to that of this research, using the sol-gel method for the preparation of silicon dioxide nanoparticles using dissolved silica gel and nitric acid for the removal of Pb(II) and Cd(II) ions in aqueous media. They prepared SiO₂ nanoparticles at three different pH values, namely 6, 7 and 8, and varied the pH as well, although they did so in a shorter range and also did not use commercial samples to make the study more extensive. They also calcined the nanoparticles at 800 °C for 2 h, a treatment not necessary or sought in this work because the use of such a high temperature will require, apart from special equipment, a large amount of energy, reducing the viability of the synthesis and therefore of the application. They found nanoparticle sizes of about 40 nm, similar in size to that estimated in this study.

In 2019, Hong et al. [45] used SiO₂ nanoparticles combined with FeO nanoparticles (10 nm) prepared by chemical vapor deposition. After the deposition of Fe oxide nanoparticles, they found an adsorption capacity of SiO₂ for methylene blue (MB) from 98 to 100% in 3 h of use. Similar results are sought, but with one less method, in addition to the fact that it is not combined with any other nanoparticle and will seek to use less time. In 2022, Ruchi et al. [46] used the same sol-gel method to synthesize TiO₂/SiO₂ nanoparticles from titanium tetra isopropoxide and tetraethoxysilane precursors; these precursors were calcined at 300 °C, 500 °C, and 800 °C. The estimated particle size was 18 nm. The nanoparticles combined TiO₂ nuclei encased within SiO₂ particles with an average crystallite size of 10–20 nm. They were evaluated for the degradation of methylene blue dyes, and it was found that the sample calcined at 300 °C exhibited a better photodegradation of 85% in 2 h. Similar results are expected, but they used an extra process, calcination, in addition to the fact that there was no combination with any other nanoparticle, and better results will be obtained in the adsorption ranges of 85%; for that study, it is proposed that it exceeds 95% adsorption.

In 2023, Eddy et al. [47] used the combination of TiO₂/SiO₂ nanoparticles in the coating process of polyester fabrics with the sol-gel-assisted sonochemical method. With the addition of SiO₂ with an equal or greater proportion of TiO₂, the occurrence of agglomeration on the dye surface increased. The tests on the degradation of the dyes gave a 97% expected result for this study, but without the combination of nanoparticles or synthesis techniques. In 2018, Aly et al. [34] used SiO₂ nanoparticles in removal of methylene blue dye under an ultraviolet light source. They found that the dye degraded completely within 90 s, using 10 g/L of SiO₂ nanoparticles at pH 1.5 and 11. Although this study is similar to the one in this article because of the variation in the pH, it cannot be compared in the use

for removing dye due to the difference in the amount that was used, and this uses $1000\times$ of material, so there is no comparison; what can be highlighted in this study is that, using UV-vis spectroscopy, they mention that there is photocatalysis, like Nandanwar et al. [34] who, in 2015, used the sol-gel method and TEOS for the synthesis of SiO_2 nanoparticles combined with calcination at $300\text{ }^\circ\text{C}$ for the degradation of methylene blue through the photocatalytic activity of SiO_2 . No evidence of photocatalytic properties of SiO_2 nanoparticles was found in this study.

Here, MB was used, but other investigations in the comparison used methyl orange (MO) and MB and SiO_2 nanoparticles as catalysts for photocatalysis in the presence of UV light, obtaining similar results for both colorants. And these results were similar to ours with MB. It was observed that catalyst doses significantly affect the photocatalytic degradation of MO and MB. The maximum degradation efficiency of the dye was achieved with the combination of UV in the presence of SiO_2 nanoparticles. Hence, from experimental results, it was found that the silica nanoparticles enhanced the photocatalytic activity under UV and were cost-effectively employed for the degradation of dye effluent with little more retention time against methylene blue and methyl orange dye, which agrees with our results using only MB dye [48].

5. Conclusions

SiO_2 nanoparticles were synthesized effectively by the sol-gel method using sodium silicate (Na_2SiO_3) as solvents without using TEOS, which makes it an ecological and low-cost method.

XRD analysis of the nanoparticles indicates the presence of the amorphous phase with the diffraction angle of $2\theta = 23^\circ$, which is the main characteristic associated with SiO_2 . The results of the characterization by UV-Vis spectroscopy show that the nanoparticles have an absorbance value in the region of 200 nm to 300 nm, showing that the material possesses the nature associated with SiO_2 nanoparticles.

The main factors affecting the SiO_2 nanoparticles are temperature, pH value, and salinity. In addition, other factors such as the shape, size, porosity, and morphology of the nanoparticles may also play a role. The three types of SiO_2 nanoparticles do not show a notable difference in the pH range between 5 and 7, although there is a difference as can be seen from Table 2; at low amounts of SiO_2 nanoparticles (10 mg), the yield of the MB degradation reaction is higher at pH 7 than at pH 5, approximately 20% to 30%.

The application of SiO_2 nanoparticles as a nanoadsorbent for the removal of dyes was verified by means of UV-Vis spectroscopy, and this was reflected by the removal of methylene blue. It was found that the nanoparticles with the best performance were those that were synthesized successfully with pH 7; they showed a 97% removal, compared to the 89% removal shown by the commercial nanoparticles.

The size of the synthesized SiO_2 nanoparticles was 60 nm smaller than that of the commercial ones, so the specific surface area of the synthesized particles is greater than $90\text{ m}^2/\text{g}$, while the commercial ones have a specific surface area of $70\text{ m}^2/\text{g}$. The shape of the synthesized particles is quasispheroidal, and their purity is 98.1%.

Studies of future interest and limitations are as follows: We consider the possibility of realizing novel studies of antibiotics that are often ineffective against Gram-negative bacteria due to their double cell membrane structure, which blocks many key antibiotics like vancomycin. Novel studies have developed hybrid silica nanoparticles that combine membrane-targeting groups with encapsulated antibiotics and a ruthenium luminescent tracking agent for optical detection. These nanoparticles have successfully delivered vancomycin and shown efficacy against various Gram-negative bacteria. The luminescence confirms the penetration of nanoparticles into bacterial cells. Modified nanoparticles with aminopolycarboxylate chelating groups effectively inhibit bacterial growth, providing a new platform for delivering antibiotics that cannot penetrate bacterial membranes on their own [49,50].

Author Contributions: Conceptualization, N.E.-V. and E.G.-M.; methodology, N.E.-V. and E.G.-M.; validation, N.E.-V. and V.M.C.; formal analysis, A.M.G.-H. and M.G.-M.; investigation, N.E.-V., M.G.-M. and M.G.-P.; resources, N.E.-V., C.G.-R. and M.G.-M.; data curation, E.G.-M.; writing—original draft preparation, N.E.-V. and E.G.-M.; writing—review and editing, E.G.-M., N.E.-V., V.M.C. and M.G.-P.; visualization, M.G.-P. and E.G.-M.; supervision, V.M.C.; project administration N.E.-V. and C.G.-R.; funding acquisition, N.E.-V., A.M.G.-H. and M.G.-M. All authors have read and agreed to the published version of the manuscript.

Funding: This research was supported by the Facultad de Ciencias Físico Matemáticas of the Universidad Autónoma de Nuevo León with assistance from Dr. Atilano Martínez Huerta and Dr. José Apolinar Loyola Rodríguez.

Data Availability Statement: The datasets used during the current study are available from the corresponding author.

Acknowledgments: The authors are thankful for the support for the publication from the Project of Programa de Apoyo a la Investigación Científica y Tecnológica (PAICYT) given by Dirección de Investigación of Universidad Autónoma de Nuevo León.

Conflicts of Interest: The authors declare no conflicts of interest.

References

1. Mohajerani, A.; Burnett, L.; Smith, J.V.; Kurmus, H.; Milas, J.; Arulrajah, A.; Horpibulsuk, S.; Abdul Kadir, A. Nanoparticles in construction materials and other applications, and implications of nanoparticle use. *Materials* **2019**, *12*, 3052. [[CrossRef](#)] [[PubMed](#)]
2. Khajeh, M.; Laurent, S.; Dastafkan, K. Nanoadsorbents: Classification, preparation, and applications (with emphasis on aqueous media). *Chem. Rev.* **2013**, *113*, 7728–7768. [[CrossRef](#)] [[PubMed](#)]
3. Mahmoudi, M.; Bouras, O.; Hadjersi, T.; Baudu, M.; Aissiou, S. Synthesis of CuO-modified silicon nanowires as a photocatalyst for the degradation of malachite green. *React. Kinet. Mech. Catal.* **2021**, *134*, 971–987. [[CrossRef](#)]
4. Akhter, F.; Rao, A.A.; Abbasi, M.N.; Ahmed Wahocho, S.; Mallah, M.A.; Anees-ur-Rehman, H.; Chandio, Z.A. A Comprehensive Review of Synthesis, Applications and Future Prospects for Silica Nanoparticles (SNPs). *Silicon* **2022**, *14*, 8295–8310. [[CrossRef](#)]
5. Bhatnagar, A.; Vilar, V.J.P.; Botelho, C.M.; Boaventura, R.A.R. Recent advances in nano-adsorbents for water treatment. *Environ. Chem. Lett.* **2022**, *20*, 125–145. [[CrossRef](#)]
6. Jain, K.; Patel, A.S.; Pardhi, V.P.; Flora, S.J.S. Nanotechnology in Wastewater Management: A New Paradigm Towards Wastewater Treatment. *Molecules* **2021**, *26*, 1797. [[CrossRef](#)] [[PubMed](#)]
7. Benhadria, N.; Hachemaoui, M.; Zaoui, F.; Mokhtar, A.; Boukreris, S.; Attar, T.; Belarbi, L.; Boukoussa, B. Catalytic reduction of methylene blue dye by copper oxide nanoparticles. *J. Clust. Sci.* **2022**, *33*, 249–260. [[CrossRef](#)]
8. Manasa, R.L.; Mehta, A. Wastewater: Sources of Pollutants and Its Remediation. In *Environmental Biotechnology*; Gothandam, K., Ranjan, S., Dasgupta, N., Lichtfouse, E., Eds.; Environmental Chemistry for a Sustainable World, Vol 45.; Springer: Cham, Switzerland, 2020; Volume 2. [[CrossRef](#)]
9. Jesús Ruíz-Baltazar, Á.; Reyes-López, S.Y.; de Lourdes Mondragón-Sánchez, M.; Robles-Cortés, A.I.; Pérez, R. Eco-friendly synthesis of Fe₃O₄ nanoparticles: Evaluation of their catalytic activity in methylene blue degradation by kinetic adsorption models. *Results Phys.* **2019**, *12*, 989–995. [[CrossRef](#)]
10. Cheng, K.; Heng, S.; Tieng, S.; David, F.; Dine, S.; Haddad, O.; Colbeau-Justin, C.; Traore, M.; Kanaev, A. Mixed Metal Oxide W-TiO₂ Nanopowder for Environmental Process: Synergy of Adsorption and Photocatalysis. *Nanomaterials* **2024**, *14*, 765. [[CrossRef](#)] [[PubMed](#)]
11. George, A.; Raj, D.M.A.; Venci, X.; Raj, A.D.; Irudayaraj, A.A.; Josephine, R.L.; Sundaram, S.J.; Al-Mohaimed, A.M.; Al Farraj, D.A.; Chen, T.-W.; et al. Photocatalytic effect of CuO nanoparticles flower-like 3D nanostructures under visible light irradiation with the degradation of methylene blue (MB) dye for environmental application. *Environ. Res.* **2022**, *203*, 111880. [[CrossRef](#)] [[PubMed](#)]
12. Modi, S.; Yadav, V.K.; Gacem, A.; Ali, I.H.; Dave, D.; Khan, S.H.; Yadav, K.K.; Rather, S.-u.; Ahn, Y.; Son, C.T.; et al. Recent and emerging trends in remediation of methylene blue dye from wastewater by using zinc oxide nanoparticles. *Water* **2022**, *14*, 1749. [[CrossRef](#)]
13. Suvith, V.S.; Philip, D. Catalytic degradation of methylene blue using biosynthesized gold and silver nanoparticles. *Spectrochim. Acta Part A Mol. Biomol. Spectrosc.* **2014**, *118*, 526–532. [[CrossRef](#)] [[PubMed](#)]
14. Ceroni, L.; Benazzato, S.; Pressi, S.; Calvillo, L.; Marotta, E.; Menna, E. Enhanced Adsorption of Methylene Blue Dye on Functionalized Multi-Walled Carbon Nanotubes. *Nanomaterials* **2024**, *14*, 522. [[CrossRef](#)] [[PubMed](#)]
15. Kumari, P.; Alam, M.; Siddiqi, W.A. Usage of nanoparticles as adsorbents for waste water treatment: An emerging trend. *Sustain. Mater. Technol.* **2019**, *22*, e00128. [[CrossRef](#)]
16. Crini, G.; Lichtfouse, E. Advantages and disadvantages of techniques used for wastewater treatment. *Environ. Chem. Lett.* **2019**, *17*, 145–155. [[CrossRef](#)]

17. Qi, D.; Lin, C.; Zhao, H.; Liu, H.; Lü, T. Size regulation and prediction of the SiO₂ nanoparticles prepared via Stöber process. *J. Dispers. Sci. Technol.* **2017**, *38*, 70–74. [[CrossRef](#)]
18. Zaheer, S.; Shehzad, J.; Chaudhari, S.K.; Hasan, M.; Mustafa, G. Morphological and Biochemical Responses of *Vigna radiata* L. Seedlings Towards Green Synthesized SiO₂ NPs. *Silicon* **2023**, *15*, 5925–5936. [[CrossRef](#)]
19. Rahimzadeh, C.Y.; Barzinjy, A.A.; Mohammed, A.S.; Hamad, S.M. Green synthesis of SiO₂ nanoparticles from *Rhus coriaria* L. Extract: Comparison with chemically synthesized SiO₂ nanoparticles. *PLoS ONE* **2022**, *17*, e0268184. [[CrossRef](#)] [[PubMed](#)]
20. Post, P.; Wurlitzer, L.; Maus-Friedrichs, W.; Weber, A.P. Characterization and applications of nanoparticles modified in-flight with silica or silica-organic coatings. *Nanomaterials* **2018**, *8*, 530. [[CrossRef](#)] [[PubMed](#)]
21. Sharma, P.; Kherb, J.; Prakash, J.; Kaushal, R. A novel and facile green synthesis of SiO₂ nanoparticles for removal of toxic water pollutants. *Appl. Nanosci.* **2023**, *13*, 735–747. [[CrossRef](#)]
22. Abuzeid, H.M.; Julien, C.M.; Zhu, L.; Hashem, A.M. Green Synthesis of Nanoparticles and Their Energy Storage, Environmental, and Biomedical Applications. *Crystals* **2023**, *13*, 1576. [[CrossRef](#)]
23. Vijayaram, S.; Razafindralambo, H.; Sun, Y.Z.; Vasantharaj, S.; Ghafarifarsani, H.; Hoseinifar, S.H.; Raeeszadeh, M. Applications of Green Synthesized Metal Nanoparticles—A Review. *Biol. Trase Elem. Res.* **2024**, *202*, 360–386. [[CrossRef](#)] [[PubMed](#)]
24. Jimenez-Vivanco, M.R.; García, G.; Carrillo, J.; Morales-Morales, F.; Coyopol, A.; Gracia, M.; Doti, R.; Faubert, J.; Lugo, J.E. Porous Si-SiO₂ UV microcavities to modulate the responsivity of a broadband photodetector. *Nanomaterials* **2020**, *10*, 222. [[CrossRef](#)]
25. Ghufuran, M.; Huitink, D. Synthesis of nano-size paraffin/silica-based encapsulated phase change materials of high encapsulation ratio via sol-gel method. *J. Mater. Sci.* **2023**, *58*, 7673–7689. [[CrossRef](#)]
26. Shi, B.; Xie, L.; Ma, B.; Zhou, Z.; Xu, B.; Qu, L. Preparation and properties of highly transparent SiO₂ aerogels for thermal insulation. *Gels* **2022**, *8*, 744. [[CrossRef](#)] [[PubMed](#)]
27. Alavi, M.; Hamblin, M.R.; Mozafari, M.R.; Rose Alencar De Menezes, I.; Douglas Melo Coutinho, H. Surface modification of SiO₂ nanoparticles for bacterial decontaminations of blood products. *Cell. Mol. Biomed. Rep.* **2022**, *2*, 87–97. [[CrossRef](#)]
28. Sun, J.; Xu, Z.; Li, W.; Shen, X. Effect of nano-SiO₂ on the early hydration of alite-sulphoaluminate cement. *Nanomaterials* **2017**, *7*, 102. [[CrossRef](#)] [[PubMed](#)]
29. Gomes, B.R.; Lopes, J.L.; Coelho, L.; Ligonzo, M.; Rigoletto, M.; Magnacca, G.; Deganello, F. Development and Upscaling of SiO₂@TiO₂ Core-Shell Nanoparticles for Methylene Blue Removal. *Nanomaterials* **2023**, *13*, 2276. [[CrossRef](#)] [[PubMed](#)]
30. Mikhnenko, M.D.; Cherepanova, S.V.; Gerasimov, E.Y.; Pochtar, A.A.; Alekseeva (Bykova), M.V.; Kukushkin, R.G.; Yakovlev, V.A.; Bulavchenko, O.A. Defect Structure of Nanocrystalline NiO Oxide Stabilized by SiO₂. *Inorganics* **2023**, *11*, 97. [[CrossRef](#)]
31. Eissa, D.; Hegab, R.H.; Abou-Shady, A.; Kotp, Y.H. Green synthesis of ZnO, MgO and SiO₂ nanoparticles and its effect on irrigation water, soil properties, and *Origanum majorana* productivity. *Sci. Rep.* **2022**, *12*, 5780. [[CrossRef](#)] [[PubMed](#)]
32. Imoisili, P.E.; Nwanna, E.C.; Jen, T.-C. Facile Preparation and Characterization of Silica Nanoparticles from South Africa Fly Ash Using a Sol-Gel Hydrothermal Method. *Processes* **2022**, *10*, 2440. [[CrossRef](#)]
33. Aly, H.F.; Abd-Elhamid, A.I. Photocatalytic degradation of methylene blue dye using silica oxide nanoparticles as a catalyst. *Water Environ. Res.* **2018**, *90*, 807–817. [[CrossRef](#)]
34. Nandanwar, R.; Singh, P.; Haque, F.Z. Synthesis and characterization of SiO₂ nanoparticles by sol-gel process and its degradation of methylene blue. *Am. Chem. Sci. J.* **2015**, *5*, 1–10. [[CrossRef](#)]
35. Zhu, Z.; Liang, H.; Sun, D.W. Infusing silicone and camellia seed oils into micro-/nanostructures for developing novel anti-icing/frosting surfaces for food freezing applications. *ACS Appl. Mater. Interfaces* **2023**, *15*, 14874–14883. [[CrossRef](#)]
36. Jain, A.; Wadhawan, S.; Mehta, S.K. Biogenic synthesis of non-toxic iron oxide NPs via *Syzygium aromaticum* for the removal of methylene blue. *Environ. Nanotechnol. Monit. Manag.* **2021**, *16*, 100464. [[CrossRef](#)]
37. Sharma, P.; Prakash, J.; Kaushal, R. An insight into the green synthesis of SiO₂ nanostructures as a novel adsorbent for removal of toxic water pollutants. *Environ. Res.* **2022**, *212*, 113328. [[CrossRef](#)] [[PubMed](#)]
38. Babyszko, A.; Wanag, A.; Kusiak-Nejman, E.; Morawski, A.W. Effect of Calcination Temperature of SiO₂/TiO₂ Photocatalysts on UV-VIS and VIS Removal Efficiency of Color Contaminants. *Catalysts* **2023**, *13*, 186. [[CrossRef](#)]
39. Chen, Q.; Xue, X.; Liu, Y.; Guo, A.; Chen, K.; Yin, J.; Yu, F.; Zhu, H.; Guo, X. Shear-induced fabrication of SiO₂ nano-meshes for efficient uranium capture. *J. Hazard. Mater.* **2022**, *438*, 129524. [[CrossRef](#)] [[PubMed](#)]
40. Alonso-De la Garza, D.A.; Guzmán, A.M.; Gómez-Rodríguez, C.; Martínez, D.I.; Elizondo, N. Influence of Al₂O₃ and SiO₂ nanoparticles addition on the microstructure and mechano-physical properties of ceramic tiles. *Ceram. Int.* **2022**, *48*, 12712–12720. [[CrossRef](#)]
41. Rong, Z.; Zhao, M.; Wang, Y. Effects of modified nano-SiO₂ particles on properties of high-performance cement-based composites. *Materials* **2020**, *13*, 646. [[CrossRef](#)] [[PubMed](#)]
42. Dehsheikh, H.G.; Ghasemi-Kahrizsangi, S. The influence of silica nanoparticles addition on the physical, mechanical, thermo-mechanical as well as microstructure of Mag-Dol refractory composites. *Ceram. Int.* **2017**, *43*, 16780–16786. [[CrossRef](#)]
43. Wardiyati, S.; Adi, W.A. Synthesis and characterization of microwave absorber SiO₂ by sol-gel method. In *IOP Conference Series: Materials Science and Engineering*; IOP Publishing: Bristol, UK, 2017; Volume 202, p. 012059. [[CrossRef](#)]
44. El-Feky, H.H.; Behiry, M.S.; Amin, A.S.; Nassar, M.Y. Facile fabrication of nano-sized SiO₂ by an improved sol-gel route: As an adsorbent for enhanced removal of Cd (II) and Pb (II) ions. *J. Inorg. Organomet. Polym. Mater.* **2022**, *32*, 1129–1141. [[CrossRef](#)]
45. Hong, Y.; Cha, B.J.; Kim, Y.D.; Seo, H.O. Mesoporous SiO₂ particles combined with Fe oxide nanoparticles as a regenerative methylene blue adsorbent. *ACS Omega* **2019**, *4*, 9745–9755. [[CrossRef](#)] [[PubMed](#)]

46. Ruchi, N.; Bamne, J.; Singh, N.; Sharma, P.K.; Singh, P.; Umar, A.; Haque, F.Z. Synthesis of titania/silica nanocomposite for enhanced photodegradation of methylene blue and methyl orange dyes under uv and mercury lights. *ES Mater. Manuf.* **2022**, *16*, 78–88. [[CrossRef](#)]
47. Eddy, D.R.; Luthfiah, A.; Permana, M.D.; Deawati, Y.; Firdaus, M.L.; Rahayu, I.; Izumi, Y. Rapid Probing of Self-Cleaning Activity on Polyester Coated by Titania–Natural Silica Nanocomposite Using Digital Image-Based Colorimetry. *ACS Omega* **2023**, *8*, 7858–7867. [[CrossRef](#)] [[PubMed](#)]
48. Biradar, A.I.; Sarvalkar, P.D.; Teli, S.B.; Pawar, C.A.; Patil, P.S.; Prasad, N.R. Photocatalytic degradation of dyes using one-step synthesized silica nanoparticles. *Mater. Today Proc.* **2021**, *43*, 2832–2838. [[CrossRef](#)]
49. Muguruza, A.R.; di Maio, A.; Hodges, N.J.; Blair, J.M.; Pikramenou, Z. Chelating silica nanoparticles for efficient antibiotic delivery and particle imaging in Gram-negative bacteria. *Nanoscale Adv. R. Soc. Chem.* **2023**, *5*, 2453–2461. [[CrossRef](#)] [[PubMed](#)]
50. Song, Y.; Zheng, X.; Hu, J.; Ma, S.; Li, K.; Chen, J.; Xu, X.; Lu, X.; Wang, X. Recent advances of cell membrane-coated nanoparticles for therapy of bacterial infection. *Front. Microbiol.* **2023**, *14*, 3428. [[CrossRef](#)]

Disclaimer/Publisher’s Note: The statements, opinions and data contained in all publications are solely those of the individual author(s) and contributor(s) and not of MDPI and/or the editor(s). MDPI and/or the editor(s) disclaim responsibility for any injury to people or property resulting from any ideas, methods, instructions or products referred to in the content.